VARIATION OF STRUCTURAL FEATURES AND INTERACTIONS WITH SUBSTITUTION OF DIFFERENT ALKYL FOR IMIDAZOLIUM BASED ILS

Abstract

The drastic difference in melting point of Ionic Liquid was observed with a small change in cation structure. The conformation of 1-crotyl -3-methyl imidazolium hexafluorophosphate (cmimPF6) has been identified with the help of Raman marker bands and compared with the 1-butyl-3-methyl imidazolium hexafluorophosphates (bmimPF6). Multiple interactions between cation and anion in cmimPF6 are observed using DFT calculation. Raman band involving C2-H was found to be strongly influenced by interaction with anion.Hydrogen bonding at C2-H is found to be very important but not the sole determining physical property of ILs. A new interaction involving C2---F is identified for the first time using the DFT method. It appears that multiple weak interactions have profound effects on the physical state of an ionic liquid. Hence a small change in cation was found to make a drastic change in the physical state of the ILs as evident from our comparative studies of saturated and unsaturated alkyl chains containing imidazolium ILs.

Keywords: Ionic liquids, Hydrogen bonding interaction, DFT calculation, NBO Analysis, melting point

Authors

Ravi Ranjan
Department of Chemistry
Gram Bharti College
Ramgarh, Kaimur
Veer Kunwar Singh University
India.

Madhulata Shukla
Department of Chemistry
Gram Bharti College
Ramgarh, Kaimur
Veer Kunwar Singh University
India.
madhu1.shukla@gmail.com

Copyright © 2024 Authors

I. INTRODUCTION

In the last three decades, ionic liquids (ILs) have been the hot topic of research in the field of academia as well as industries. It is predominantly due to its exceptional characteristics and properties of low vapor pressure, high thermal stability, recyclability, and low toxicity. These liquids are accepted as green and sustainable liquids with abundant potential to be used in a large number of applications. Ionic Liquidsare considered to be new materials and have been the subject of comprehensive experimental and theoretical studies due to their unique solvent properties and are used in a wide range of applications in substitution of conventional organic solvents.[1-4]Due to the non-toxic, non-volatile, and non-flammable nature of the IL, it is used in different kinds of synthesis, electrochemistry,[5] catalysis,[6]separate techniques,[7-8]and many more applications.[9–15]A great emphasis is placed on the ability to design and select novel ILs with properties tuned for certain applications. Mainly, ILs are classified into four different types of cations namely alkylammonium-, dialkyl imidazolium-, phosphonium-, and lastly N-alkylpyridinium-based ILs. With these cations, different numbers of anions are combined in numerous permutations and combinations ways to produce millions of ion pairs.

Due to various permutations and combinations of cation and anion, it is defined to be a designer solvent.[16]The liquid nature of ILs over a wide range of temperatures and slight vapor pressure makes IL suitable for its application as a solvent in different fields such as nanoparticle synthesis, organic synthesis, and various extraction processes involved in industries.[17-18]The properties of any material are closely related to its molecular structure. It is crucial to have a deep understanding of the structural features of a material to comprehend its properties. Theoretical calculations are an essential tool in determining the structures of liquids. Density Functional Theory (DFT) is a popular and versatile method used in computational Physics and Chemistry to find out the electronic and thermo physical properties of materials. This method is based on the idea that the energy of a system can be determined by knowing its electron density. DFT has become increasingly popular over the years due to its accuracy and efficiency in predicting the properties of materials. It has been used in various fields such as materials science, solid-state physics, and chemistry. This method can also be used to study the behavior of materials under different conditions, such as temperature and pressure. Overall, the use of theoretical calculations and DFT in particular, has revolutionized the way we study materials and their properties. With its accuracy and versatility, it has become an essential tool in modern-day research.[19,20,21] DFT calculations fairly predict the isolated IL structures, vibrational modes and as well as its thermal properties.[15,22]

In this paper, the synthesis of1-crotyl-3-methyl imidazolium chloride (cmimCl),1-crotyl-3-methyl imidazolium hexafluorophosphate (cmimPF6)and 1-butyl-3-metyl imidazolium hexafluorophosphates (bmimPF6) has been reported.A systematic study of different types of specific and non-specific interactions present between ions of bmimPF6 and cmimPF6 has been reported to analyze the difference in the physical properties of these ILs. Thermal behaviour of hexafluorophosphate based ILs studied using the DTA method. cmimPF6 IL was found to be solid whereas bmimPF6exists as a liquid phase at room temperature. With the incorporation of unsaturation into the butyl group, it makes room temperature ionic liquid (RTIL) solid. This can be justified by the fact the unsaturation causes more interaction with counter anion compared to the saturated alkyl chain. Details of strength

Copyright © 2024 Authors

and type of interaction between cation and anion in an ILhave been obtained from NBO analysis of DFT optimized structures and found to explain the melting temperature of ionic liquids very well as reported by us for different ILs in our previous report.[21]Recent comparative studies of saturated and unsaturated alkyl chains containing imidazolium-based ionic liquid have revealed that even small changes in cation can have a drastic impact on the physical state of the ILs. The second-order perturbation stabilization energy was calculated using DFT and NBO analysis, providing in-depth details on the type and strength of interaction between cation and anion. These findings highlight the importance of carefully selecting the cation when designing new ionic liquids, as even subtle changes can significantly affect their properties and applications. Further research in this area may lead to the development of more efficient and effective ionic liquids for a wide range of industrial and scientific purposes. Further, experimental Raman Spectra bands have been compared with DFT calculated Raman band to analyze the different types of interaction present between cation and anion ion pair of bmimPF6 and cmimPF6. A comparison of Raman spectra of bmimPF6 and cmimPF6 ILs has been done to point out the differences present in these ILs which is responsible for the drastic change in the physical behavior of these two ILs. Different molecular orbital (HOMO –LUMO) has been calculated to get the detailed interaction and a charge transfer study has been done by analyzing the Mulliken Charge distribution in cmimPF6 and bmimPF6 ion pair

II. METHODOLOGY

1. **Reagents and Instrumentation:** The N-methylimidazole (Sigma Aldrich, redistilled, >99%), cholorobutane, crotyl chloride (Merck, Germany) was used as received for the synthesis.Acetonitrile (ACN) (HPLC grade) was procured from Merck, Germany while diethyl ether and ethyl acetate (LR grade) were obtained from Merck, India, and were used after purification following standard procedures. The infrared spectrum was measured with a Varian FTIR 3100 spectrometer in the region 400 cm^{-1}–4000cm^{-1} (having a resolution of 4 cm^{-1}) usinga neat sample. 300MHz NMR (JEOL) was used to measure the ^{1}H NMR. TGA was performed using Perkin-Elmer STA 6000 instrument under a nitrogen atmosphere at the heating rate of 10°C/min.

2. **Synthesis**

- **Synthesis of 1-Crotyl-3-Methyl Imidazolium Chloride:** 250 mL round bottom flask was taken and added 30mL dry ACN and then dissolved 7.4 mL of methyl imidazole was in it at $0^{\circ}C$ by an ice bath and added 10.0 mLof crotyl chloride in the stirring solution of methyl imidazole was under N_2 atmosphere.Stirringwas done for 5-6 hrs at 0-$5^{\circ}C$ and then kept it stirring at room temperature for 65 hrs in between TLC of the mixture was checked regularly, and finally evaporated the ACN on rotavapor, washed the ILwas with ethyl acetate (250ml X 5) and diethyl ether (100ml X 3) and then put in on high vacuum. Synthesized 1-crotyl-3-methyl imidazolium chloride (cmimCl) was purified by activated charcoal to remove color impurities.Yield=92%^{1}H NMR, (in CDCl3,δ ppm) 1.73(m), 3.69 (s), 4.89(t), 5.61(m), 5.95(m), 7.5(s), 7.75(s), 10.1(s). FTIR (KBr, cm^{-1}): 748, 1117, 1165, 1464, 1570, 2875, 2965, 3171.

- **Synthesis of 1-Crotyl -3-Methyl Imidazolium Hexa Fluorophosphates:** 1.88 g of cmimcl was taken and dissolved in 2 mL of water and then added 2.16g of $NaPF_6$ in

Copyright © 2024 Authors

an aqueous solution.The white precipitate was formed. Stirringwas done for 3 hrs at room temperature.DCM was added to the solution as a result of which white precipitate was dissolved in it and washed the reaction mixture 3-4 times with DCM and DCM solution was washed with cold water and checked the chloride with $AgNO_3$ and DCM was dried with anhydrous $MgSO_4$.A colourless solid was obtained.Yield is 80% ^{1}H NMR, (in CDCl3,δ ppm) 1.57(m), 3.82 (s), 4.59(t), 5.56(m), 5.91(m), 7.3(s), 7.38(s), 8.33(s). FTIR (KBr, cm^{-1}): 749, 835 (P-F stretching), 1117, 1165, 1464, 1570, 2877, 2960, 3164.

- **Synthesis of 1-Butyl-3-Methyl Imidazolium Hexafluro Phosphate:** $bmimPF_6$ was synthesizedfrom bmimCl as reported by us elsewhere.[15]A schematic diagram for bmimPF6 and cmimPF6 has been shown in Figure 1.

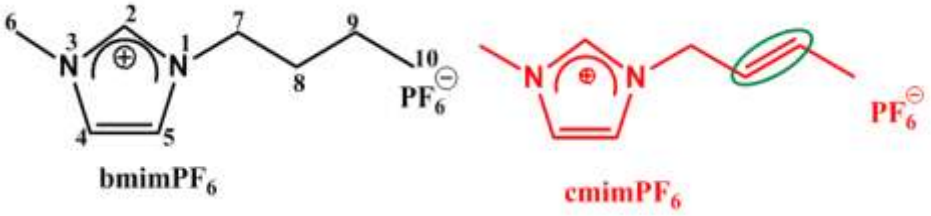

Figure 1: Schematic diagram for bmimPF6 and cmimPF6

2c. Computational method: The Gaussian 16 program [23] was used for the Density Functional Theory (DFT) calculation for bmimPF6 and cmimPF6 ILs. The basis set already implemented in the program was used for the different types of calculations. The geometries of isolated ion pairs of ILs were optimized at Becke's three-parameter hybrid method with LYP correlation (B3LYP).[24,25] 6-311G++(d,p) basis set was used for both bmimPF6 and cmimPF6. In addition to optimization, Raman frequency calculation, Natural bond orbital (NBO), and Mulliken charge distributionanalysis were also performed at the same B3LYP level of calculation using the same basis set. The absence of imaginary frequencies in the vibrational, as well as the Raman spectrum,confirms the presence of a true minimum.

III. RESULTS AND DISCUSSION

1. **Molecular Geometry Optimization and H-bonding Interaction:** Understanding the detailed information regarding the intermolecular interaction in ionic liquids it is very much important to analyze its physical properties, which is dependent upon the types and number of interactions present between the cation and anion ion pairs. Different types of interaction have different effects on ion pairs and play an important role in determining the structural, thermal, chemical, and transport properties.[27] To justify the statement that slight change in cation found to impart big changes in the physical state and properties of ILs, DFT calculation on molecular structures of $bmimPF_6$ and $cmimPF_6$ has been carried out at the B3LYP level and using the same 6-31G++(d,p) basis set in the gaseous phase to calculate the single point energy and the optimized molecular geometry. XRD coordinate of $bmimPF_6$[28]and $cmimPF_6$[29]reported elsewherewas chosen for the input file coordinates

Copyright © 2024 Authors

of cmimPF_6. The optimized molecular geometry of the cmimPF6 ion pair using DFT calculation with atoms numbered is shown in **Figure 2.**

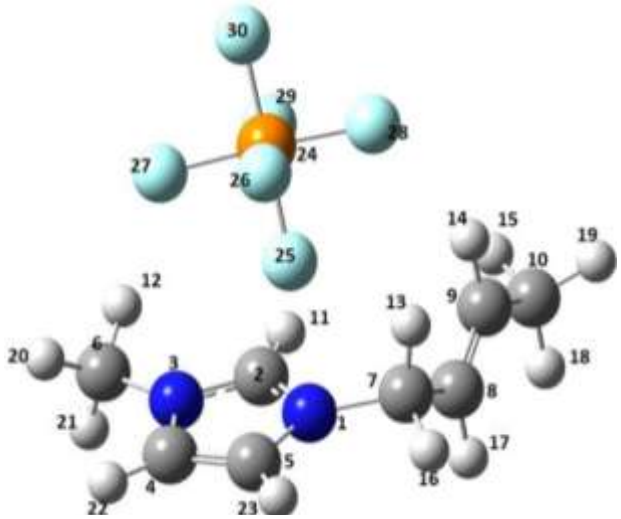

Figure 2: Optimized molecular geometry of cmimPF6 ion pair using DFT calculation

Single point energy (SPE) of the X-ray structure and energy of the optimized molecular structure of cmimPF6 (shown in **Table 1**) were found to be -1362.57 Hartee and -1362.81 Hartee respectively which varies by 0.24 Hartee (=151.857Kcal/mol), indicating that optimized structure is more stable as compared to x-ray structure.

Table 1: Comparison of geometry parameters of XRD structure and the DFT optimized structure of cmimPF6.

Parameters	X-ray Data	DFT calculated Data
SPE	-1362.57 Hartee	-1362.81 Hartee
C2-H11	0.93	1.08
C8-C9	1.33	1.34
<N1-C2-N3	109.24	108.57
<C6-N1-C2	125.86	124.67
<C8-C9-C10	124.85	125.17
<C2-N1-C7	127.58	124.33
C2-N1-C7-C8	14.03	-15.72
N1-C7-C8-C9	112.10	109.95
C7-C8-C9-C10	178.24	-179.74
N1-C2-N3-C6	-177.05	178.91
C7-N1-C2-H11	-3.168	-2.666

Also, the optimized structure of bmimBF4 and cmimBF4 was found to have energy -1364.31 and -1362.81 Hartee (shown in **Table 2**) respectively, which clearly indicates that cmimPF6 is more stable as compared to bmimPF6. The optimized structures reveal that the imidazolium ring is a planar pentagon as expected and the alkyl chain was found to exist in gauche-trans conformation and not in trans-trans.

Copyright © 2024 Authors

Table 2: Comparison of DFT optimized geometry parameters of bmimPF6 and cmimPF6

Parameters	bmimPF6	cmimPF6
Energy (Hartree)	-1364.31	-1362.81
Dipole (Debye) X= Y= Z=	-4.71 -3.24 -0.002	-4.40 -3.43 0.27
N_1-C_7	1.482Å	1.493
C_7-C_8	1.527	1.501
C_8-C_9	1.534	1.339
C_9-C_{10}	1.531	1.497
C_2-H_{11}	1.079	1.083
N_1-C_7-C_8	113.02	112.36
C_7-C_8-C_9	111.22	122.43
C_8-C_9-C_{10}	112.45	125.17
C_7-C_8-C_9-C_{10}	179.30	179.74
N_1-C_7-C_8-C_9	179.10	109.95

The optimized structure shown in **Figures 4a, 4b** and **4c**clearly shows that more Hydrogen bonding is involved in cmimPF6 as compared with that of bmimPF6. This might be the actual reason for the high melting point of cmimPF6 as compared to bmimPF6.

DFT calculated bond length C_2-H_{11} wasfound to differ by 0.154 Å from the x-ray data. C_8-C_9 bond length was found to differ by 0.011 Å. Hence the bond length in cation and anion was found to have a slight difference. While, bond angles were found to vary by approximately 1^{o}, whereas dihedral angles were found to vary with somewhat large differences. Other dihedral angles were found to vary by a maximum of 3^{o} from the experimental data. This discrepancy between experimental and calculated data is due to the fact that DFT calculation has been performed in the gaseous phase and experimental data are obtained from the crystal lattice.

2. **Comparative Study of Hydrogen Bonding Interaction In Bmimpf6 And Cmimpf6:** The difference between the molecular structure of bmimPF6 and cmimPF6 was studied using DFT calculation. Optimized parameters (bond length, bond angle, and dihedral angle), including energy and dipole moment, are tabulated in **Table 2**. Optimized geometry of bmimPF6 (shown in Figure 3(a)) and cmimPF6 (shown in Figures3(b) and 3(c)) showing hydrogen bonding interaction has been shown in Figure 3.

Copyright © 2024 Authors

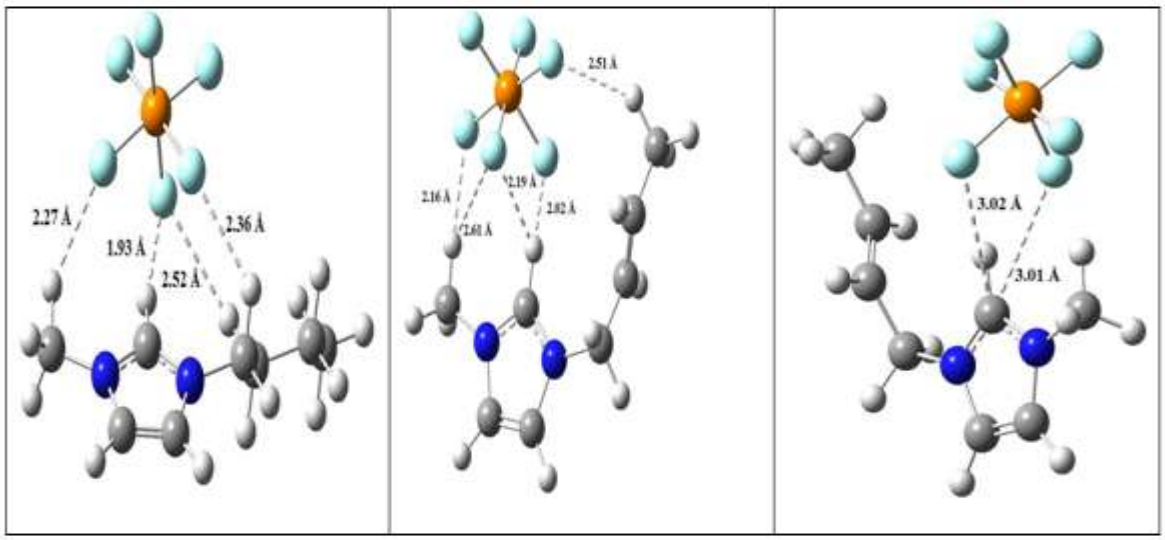

Figure 3: Optimized geometry of (a) bmimPF6 showing H-bonding interaction between H and F and (b) cmimPF6 showing H-bonding interaction between H and F(c) cmimPF6showing interaction between C and F with dotted lines.

The energy difference between the $bmimPF_6$ optimized structure and $cmimPF_6$ optimized structure was found to be 1.5 Hartee (941.3Kcal/mol) indicating that $bmimPF_6$was found to be less energetic as compared to $cmimPF_6$.

Dipole moment in X and Y directions vary slightly, whereas it varies with a significant change in the Z direction (positive in the case of $cmimPF_6$ and negative in the case of $bmimPF_6$). C_8-C_9 bond length was found to be 1.534Å (C-C) in $bmimPF_6$ and 1.339 Å (C=C) in $cmimPF_6$. C_7-C_8 bond length differs by 0.026 Å in these two ILs in the gas phase.

Other bond lengths were found to be almost similar in cation species in the gaseous phase, whereas vast differences are seen in bond angles and dihedral angles. C_7-C_8-C_9 angle found to be 111.22^o in $bmimPF_6$ and 122.43^o in $cmimPF_6$. C_8-C_9-C_{10} angle found to be 112.45^o in $bmimPF_6$ and 125.17^o in $cmimPF_6$. Similarly, a vast difference of 69.10^o is found in dihedral angle N_1-C_7-C_8-C_9,

When compared in $bmimPF_6$ and $cmimPF_6$. These differences in molecular structure lead to differences in the Physical properties of the two ILs.

Copyright © 2024 Authors

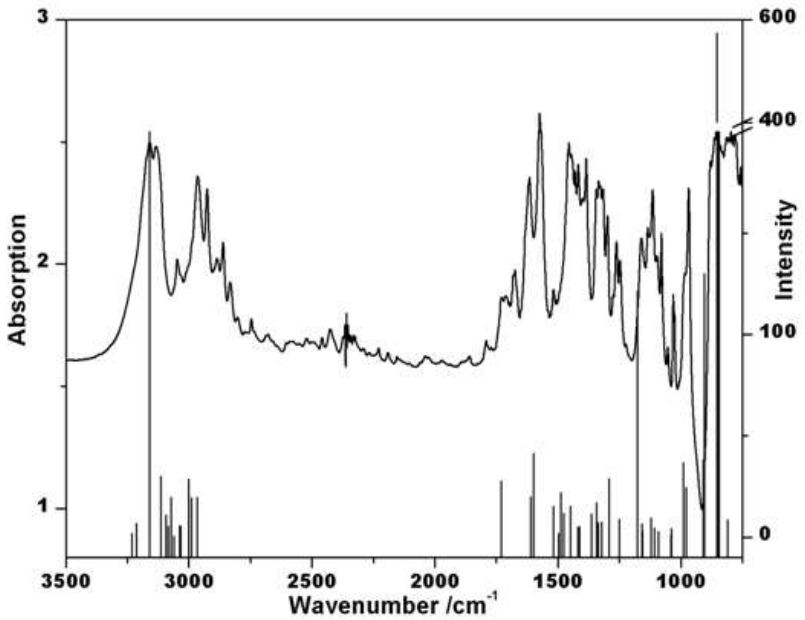

Figure 4: Correlation of experimental IR spectra of cmimPF6 with DFT calculated (vertical lines) IR frequency. A scaling factor of 0.976 was applied in a higher wavenumber region (above 2900 cm^{-1}).

3. **Analysis of Calculated IR And Raman Spectra:** IR and Raman spectra of synthesized cmimPF6 IL were recorded experimentally and correlated with DFT calculated frequencies calculated at B3LYP/6-31++G(d,p) level and have been shown in **Figure 4** and **5** respectively.

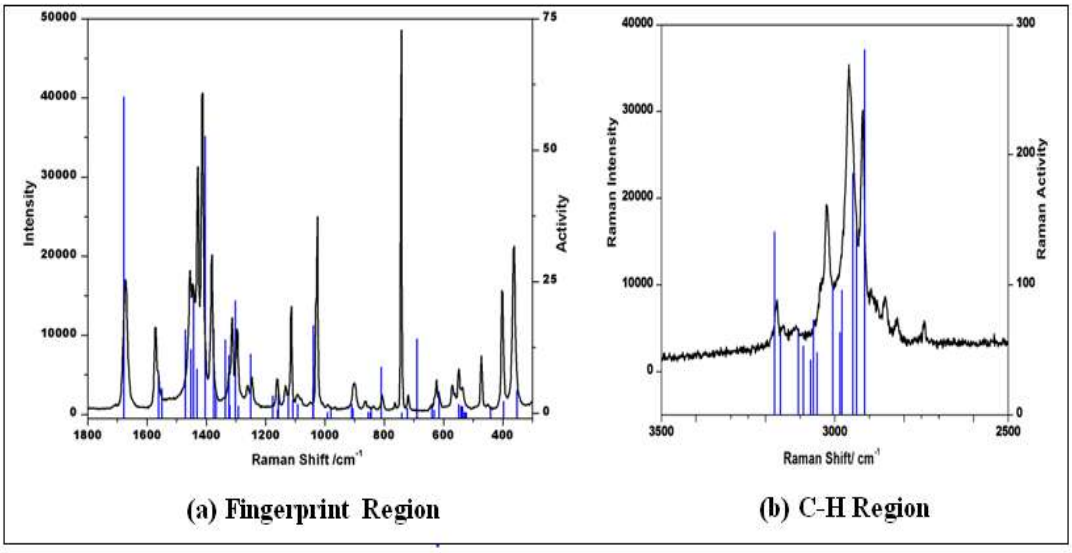

Figure 5: Correlation of Raman spectra of cmimPF6 with the DFT calculated frequency in the fingerprint region (a) at B3LYP/ 6-31++G(d,p) level. A scaling factor of 0.969 was applied above 1300 cm^{-1} in the fingerprint region and 0.959 in the C-H region (b).

Copyright © 2024 Authors

Experimental IR peaks involve intense peaks at 796, 855, 1155, 1328, 1379, 1454, 1512, 1615, 1726, 2927, 3132, and 3160 cm^{-1}. These peaks are assigned using DFT-calculated frequencies and are presented in **Table 3**. The peak at 855 $cm^{-1}$is assigned to be due to P-F stretching. 1328 and 1379 cm^{-1} peaks correspond to twisting and wagging of C-H in the crotyl group. 1615 and 1726 cm^{-1} correspond to C=C stretching in the imidazole ring and crotyl group respectively. Other 2927, 3132, and 3160 cm^{-1} peaks represent the C-H stretching in cation.DFT calculation requires a scaling factor of 0.976 in a higher wavenumber region (above 2900 cm^{-1}) to reproduce the experimental frequencies. Slight variation in higher wavenumber regions is tolerable due to the fact that experimental frequencies are anharmonic in nature while calculated frequencies are harmonic in nature.

Table 3: Selected Vibrational Frequencies and assignment of cmimPF6 and bmimPF6 moieties, showing shifting of bands for an identical vibrational motion.

cmimPF6 /cm^{-1}	**bmimPF6/cm^{-1}**	**Assignment of bands**
19	-	Calculations predict exactly the same position. Combined anion-cation libration in which equatorial F moves a larger magnitude than the axial F.
69	-	Mainly cation libration (having rocking of terminal methyl group attached with the crotyl chain)
191	-	Motion is the same as that of 69 cm-1. Looks like 2^{nd} over tone of 69 cm^{-1} band
362 (s)	-	Wagging motion involving the C=C. Since this bond is absent in bmim, the band disappears in bmimPF6.
400	414	Ip bending of C2-H and methyl group
471	472	Scissoring in PF6
536	536	P-F sym stretching, op bending of C2-H coupled with rocking of H-C-H in crotyl group
547	-	C-C=C-C scissoring
570	568	P-F scissoring
614	601	N1-C7 stretching coupled with op bending of C2-H and C5-H
630	633	Op bending (wagging) of C2-H and C4-H
721	698	C-N stretching and C2-H ip bending and C-H bending in H-C=C-H
741	741	Wagging of H-C4-C5-H
809	-	H-C=C-H twisting coupled with H-C-H rocking

Copyright © 2024 Authors

902	923	Op bending of C2-H coupled with H-C-H rocking in butyl group
991	-	H-C wagging in H-C=C-H in the crotyl group
1328	1336	Twisting of H-C in H-C=C-H
1380	-	H-C wagging in H-C=C-H in the crotyl group
1726	-	C=C stretching in crotyl gr
2914	2900	C-H sym stretching in CH2 (Bu gr)
2958	2960	C-H asym stretching in CH3
3168	3173	C- H asym stretching in H-C=C-H in ring
3238	3233	C2-H stretching

s- strong, Sym- symmetric, asym- asymmetric, str- stretching

Experimental Raman spectra of cmimPF6 consist of the intense peak at 743, 1024, 1381, 1412, 1456, 1572, 1676 cm^{-1} in the fingerprint region (**Figure 5a**) and 2920, 2960, 3022, and 3167cm^{-1} in C-H region (**Figure 5b**). C=C stretching frequency in the imidazole and crotyl group appears at 1572 and 1676 cm^{-1} respectively. Higher wavenumber peaks in Figure 4b correspond to the C-H stretching in the imidazole ring and alkyl group. A scaling factor of 0.969 has been applied above 1300 cm^{-1} in the fingerprint region and 0. 959 in the C-H region to reproduce the experimental Raman frequencies.

cmimPF6 and bmimPF6 frequencies calculated using DFT calculation on the optimized structure are reported in Table 3. Vibrational frequencies calculated using DFT, corresponding to different vibrational motions such as stretching, in-plane bending (ip) out of plane bending (op), wagging, scissoring, etc were assigned based on the predominant motion of the atoms, and the magnitude of the displacement vector associated with the atoms involved in concerned vibration and are shown in **Figure 6**. Major shifting in the peak of bmimPF6 for an identical motion w.r.t. cmimPF6 is shown by drawing the molecular vibrations, shown in **Figure 6.**

The peak at 905 cm^{-1}obtained from DFT calculation assigned to be due to out-of-plane bending of C2-H in cmimPF6 and is shifted to 923 cm^{-1} in bmimPF6, showing a deviation of 18 cm^{-1}. 991 and 1335 cm^{-1} peaks are absent in bmimPF6 which is due to wagging and in-plane bending of C-H in H-C=C-H of crotyl group. C=C stretching in crotyl group appears at 1726 cm^{-1}, which is absent in bmimPF6. All these shifting in vibrational bands are due to the presence of unequal strength of H-bonding.

Copyright © 2024 Authors

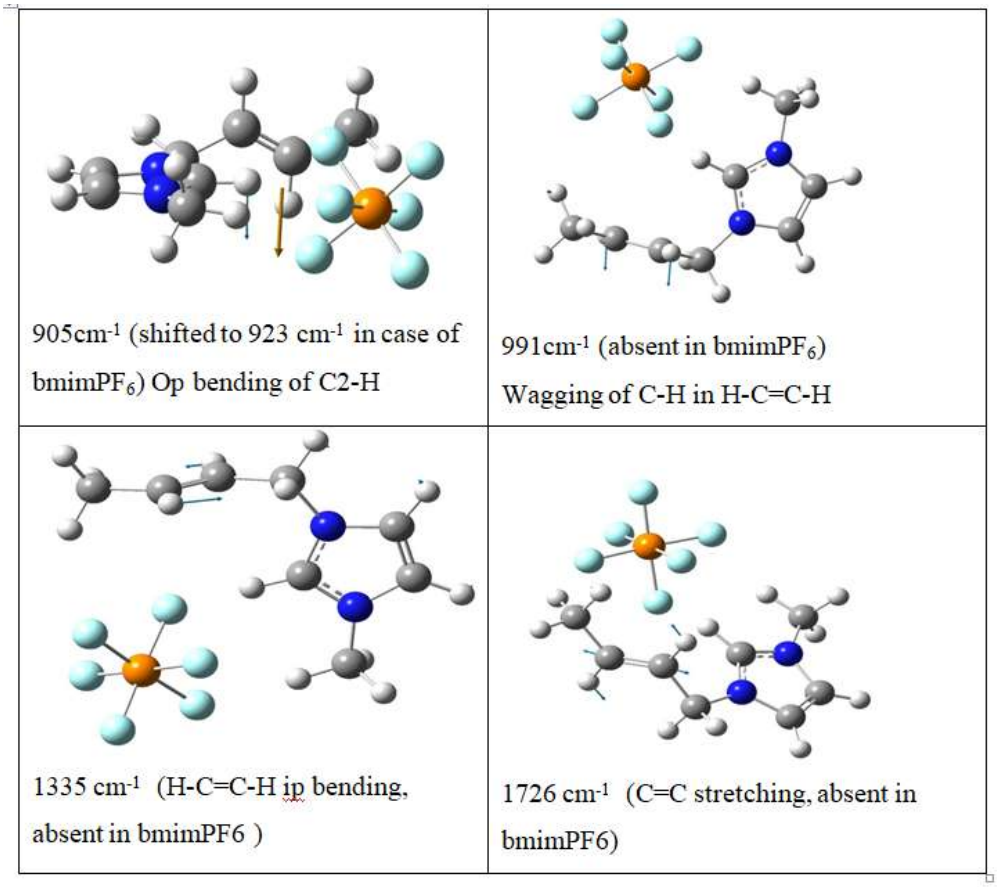

Figure 6: Few Vibrational Motions showing Shifting for bmimPF6 and cmimPF6

4. **NBO Calculation, Charge Distribution and HOMO-LUMO Presentation in Cmimpf6 And Bmimpf6 Ion Pair:** Hence a small change in cation was found to make a drastic change in the physical state of the ILs as evident from our comparative studies of saturated and unsaturated alkyl chains containing imidazolium-based ionic liquid. DFT calculation was performed to find the interactions present between the cation and anion of each ion pair. Geometry optimization of both these ion pairs indicates that a number of hydrogen bonding interactions present between cation and anion is larger in the cmimPF6 ion pair as compared to $bmimPF_6$. This higher number of interactions accounts for the higher mp of $cmimPF_6$ as compared to $bmimPF_6$ shown in Figure 4. Hence melting point of ILs observed to be reliant on both, the nature of the anion as well as alkyl chain length associated with the cation. Factors manipulating the mp observed to be: the charge distribution on ions, H-bonding, the symmetry of the ions, and the van der Waal interaction.[30,31] Natural Bond Orbital (NBO) analysis was carried out on each of the optimized structures to specify the nature of interaction present between cation and anion and the distribution of charge on ion pairs.[32] NBO charge distribution present on cmimPF6 and bmimPF6 ion pairs have been presented in **Figure 7**. It was observed that the $cmimPF_6$ ion pair has a nearly equal distribution of charge on the carbon and N atoms whereas in $bmimPF_6$, N_1, N_3, and C_8 are electron deficient (shown by green atom). This may only be due to the insertion of one double bond in the alkyl chain. Second-order perturbation stabilization energy E(2) obtained from NBO analysis of cmimPF6 and bmimPF6 has been presented in Table 4.

Copyright © 2024 Authors

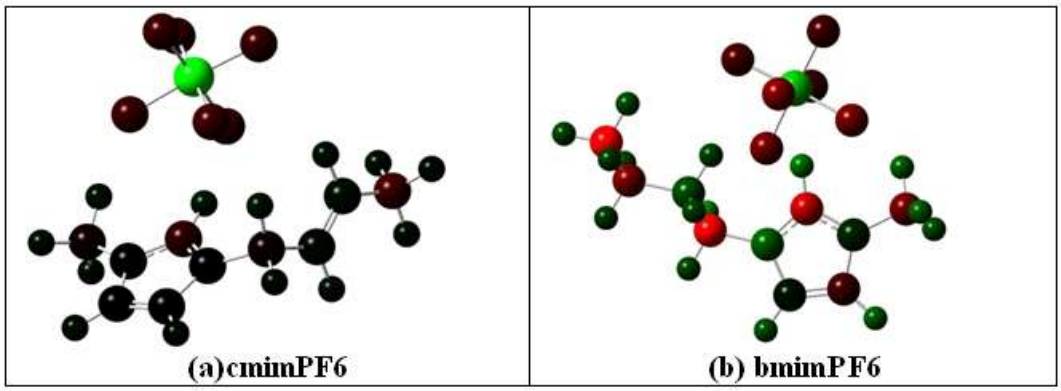

Figure 7: NBO charge distribution on cmimPF6 and bmimPF6 ion pairs. (Green color represents the most electron-deficient atom and the red color represents the most electron-rich atoms)

For cmimPF6 and bmimPF6 ILs, **E(2)** varies linearly with the melting point, similar tohalide-based ILs [21]. This trend has been verified by the similar trend of H-bonding distances between C_2-H and halide anions. Here it has been observed that E(2) value for cmimPF6 is quite larger than that of bmimPF6 and hence it directly verifies the higher melting pointof cmimPF6 than bmimPF6 as reported earlier experimentally.

Table 4: Second order perturbation stabilization energy E(2) for cmimPF6 and bmimPF6 ion pairs

ILs	E(2) for C_2-H (kcal/mol)	Total E(2) for cation anion interaction (kcal/mol)	Melting point ($^{\circ}$C) [literature]
cmimPF6	10.9	23.8	72[29]
bmimPF6	8.3	17.4	4[28]

HOMO-LUMO Representation: Pictorial representation of HOMO and LUMO of cmimPF6 and bmimPF6 has been shown in **Figure 8**. In cmimPF6 ion pair, HOMO is localized on the double bond (π (C=C)) of the crotyl group whereas LUMO (π*(Im)) is localized on the imidazole ring whereas for bmimPF6, HOMO (π(Im)) as well as LUMO (π*(Im)) both are localized on the imidazole ring. It clearly indicated that the double bond present in the crotyl group plays an important role in determining the physical properties of cmimPF6 ionic liquids.

Copyright © 2024 Authors

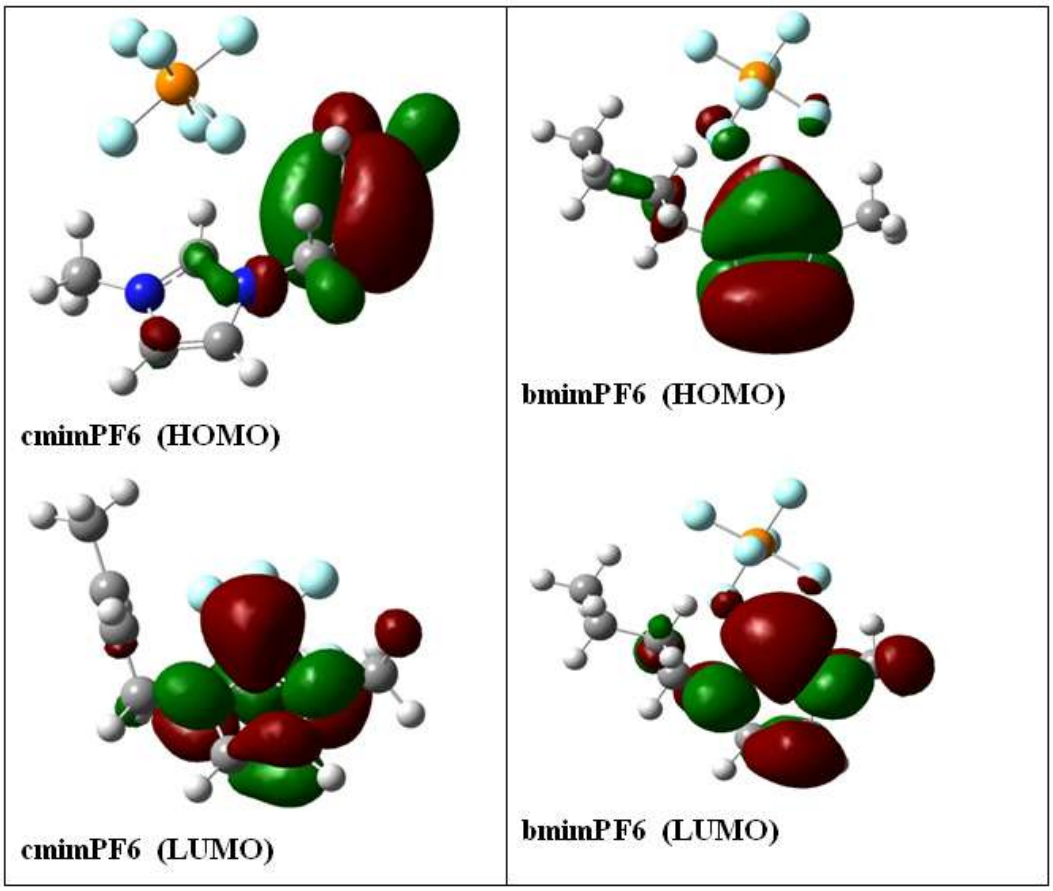

Figure 8: Pictorial representation of HOMO and LUMO of cmimPF6 and bmimPF6

IV. CONCLUSION

A small change in cation was found to make a drastic change in the physical state of the ILs as evident from our comparative studies of saturated and unsaturated containing alkyl chains. The drastic difference in mp of ILs is observed on apparently simple change in cation structure. There is no direct or specific interaction involving the C=C bond. Raman band involving C_2-H was found to be strongly influenced by interaction with anion. Multiple interactions between cation and anion in cmim$PF_6$are observed. Hydrogen bonding at C_2-H is found to be very important but not the sole determining physical property of ILs. A new interaction involving C2---F has been justified for the first time theoretically in the case of ILs. It appears that multiple weak interactions have profound effects on the physical state of an ionic liquid. Finally, the higher value of second-order perturbation stabilization energy explains clearly the higher melting point of cmimPF6 as compared to bmimPF6.

V. ACKNOWLEDGMENTS

MLS acknowledges financial assistance from UGC, India (F.30-446/2018 (BSR)). The author thanks CIF IIT(BHU) for characterization facilities and CCIS, IIT (BHU) for computational facilities.

Copyright © 2024 Authors

Conflict of Interests: The authors declare no conflict of interest.

REFERENCES

[1] Singh, S. K. & Savoy, A. W. Ionic liquids synthesis and applications: An overview. J. Mol. Liq.**297**, 112038 (2020).
[2] Welton, T. Room-Temperature Ionic Liquids. Solvents for Synthesis and Catalysis. Chem. Rev.**99**, 2071–2084 (1999).
[3] Plechkova, N. V & Seddon, K. R. Applications of ionic liquids in the chemical industry. Chem. Soc. Rev.**37**, 123–150 (2008).
[4] Anastas, P. T. & Kirchhoff, M. M. Origins, Current Status, and Future Challenges of Green Chemistry. Acc. Chem. Res.**35**, 686–694 (2002).
[5] Fuller, J., Carlin, R. T. & Osteryoung, R. A. The Room Temperature Ionic Liquid 1-Ethyl-3-methylimidazolium Tetrafluoroborate: Electrochemical Couples and Physical Properties. J. Electrochem. Soc.**144**, 3881 (1997).
[6] Chen, W., Xu, L., Chatterton, C. & Xiao, J. Palladium catalysed allylation reactions in ionic liquids. Chem. Commun. 1247–1248 (1999) doi:10.1039/A903323H.
[7] Malik, M. A., Hashim, M. A. & Nabi, F. Ionic liquids in supported liquid membrane technology. Chem. Eng. J.**171**, 242–254 (2011).
[8] Palgunadi, J., Kim, H. S., Lee, J. M. & Jung, S. Ionic liquids for acetylene and ethylene separation: Material selection and solubility investigation. Chem. Eng. Process. Process Intensif.**49**, 192–198 (2010).
[9] Kaur, G., Kumar, H. & Singla, M. Diverse applications of ionic liquids : A comprehensive review. J. Mol. Liq.**351**, 118556 (2022).
[10] Pillai, P. & Mandal, A. Synthesis and characterization of surface-active ionic liquids for their potential application in enhanced oil recovery. J. Mol. Liq.**345**, 117900 (2022).
[11] Welton, T. Ionic liquids : a brief history. 691–706 (2018).
[12] Ghandi, K. A Review of Ionic Liquids , Their Limits and Applications. (2018) doi:10.4236/gsc.2014.41008.
[13] Kaur, R., Kumar, H. & Singla, M. A thermodynamic investigation of the effect of cationic structure on the self-aggregation behavior of Surface-Active ionic liquids in the presence of an amino acid. J. Mol. Liq.**354**, 118904 (2022).
[14] Vavra, S. & Martinelli, A. Surface active alkyl-imidazolium ionic liquids studied as templates to form vertically oriented pores in silica thin films. J. Mol. Liq.**353**, 118686 (2022).
[15] Shukla, M., Srivastava, N. & Sah, S. Interactions and Transitions in Imidazolium Cation Based Ionic Liquids. Ion. Liq. - Classes Prop. (2011) doi:10.5772/23845.
[16] Fumino, K., Wulf, A. & Ludwig, R. The potential role of hydrogen bonding in aprotic and protic ionic liquids. Phys. Chem. Chem. Phys.**11**, 8790–8794 (2009).
[17] Nasirpour, N., Nasirpour, N., Mohammadpourfard, M., Mohammadpourfard, M. & Heris, S. Z. Ionic liquids: Promising compounds for sustainable chemical processes and applications. Chem. Eng. Res. \& Des.**160**, 264–300 (2020).
[18] Mittal, H., Alili, A. R. Al & Alhassan, S. M. Solid polymer desiccants based on poly(acrylic acid-co-acrylamide) and Laponite RD: Adsorption isotherm and kinetics studies. Colloids Surfaces A Physicochem. Eng. Asp.**599**, 124813 (2020).
[19] Shukla, M., Srivastava, N. & Saha, S. Theoretical and spectroscopic studies of 1-butyl-3-methylimidazolium iodide room temperature ionic liquid: Its differences with chloride and bromide derivatives. J. Mol. Struct.**975**, 349–356 (2010).
[20] Shukla, M. Hydrogen bonding interactions in nicotinamide Ionic Liquids: A comparative spectroscopic and DFT studies. J. Mol. Struct.**1131**, 275–280 (2017).
[21] Shukla, M. & Saha, S. Relationship between stabilization energy and thermophysical properties of different imidazolium ionic liquids: DFT studies. Comput. Theor. Chem.**1015**, 27–33 (2013).
[22] Shukla, M., Noothalapati, H., Shigeto, S. & Saha, S. Importance of weak interactions and conformational equilibrium in N-butyl-N-methylpiperidinium bis(trifluromethanesulfonyl) imide room temperature ionic liquids: Vibrational and theoretical studies. Vib. Spectrosc.**75**, 107–117 (2014).
[23] Frisch, M. J.; Trucks, G. W.; Schlegel, H. B.; Scuseria, G. E.; Robb, M. A.; Cheeseman, J. R.; Scalmani, G.; Barone, V.; Petersson, G. A.; Nakatsuji, H.; Li, X.; Caricato, M.; Marenich, A. V.; Bloino, J.; Janesko, B. G.; Gomperts, R.; Mennucci, B.; Hratchian, H. P.; Ortiz, J. V.; Izmaylov, A. F.; Sonnenberg, J. L.; Williams-Young, D.; Ding, F.; Lipparini, F.; Egidi, F.; Goings, J.; Peng, B.; Petrone, A.; Henderson, T.;

Copyright © 2024 Authors

Ranasinghe, D.; Zakrzewski, V. G.; Gao, J.; Rega, N.; Zheng, G.; Liang, W.; Hada, M.; Ehara, M.; Toyota, K.; Fukuda, R.; Hasegawa, J.; Ishida, M.; Nakajima, T.; Honda, Y.; Kitao, O.; Nakai, H.; Vreven, T.; Throssell, K.; Montgomery, J. A., Jr.; Peralta, J. E.; Ogliaro, F.; Bearpark, M. J.; Heyd, J. J.; Brothers, E. N.; Kudin, K. N.; Staroverov, V. N.; Keith, T. A.; Kobayashi, R.; Normand, J.; Raghavachari, K.; Rendell, A. P.; Burant, J. C.; Iyengar, S. S.; Tomasi, J.; Cossi, M.; Millam, J. M.; Klene, M.; Adamo, C.; Cammi, R.; Ochterski, J. W.; Martin, R. L.; Morokuma, K.; Farkas, O.; Foresman, J. B.; Fox, D. J.Revision C.01,Gaussian, Inc., Wallingford CT, 2016.

[24] Lee, C., Yang, W. & Parr, R. G. Development of the Colle-Salvetti correlation-energy formula into a functional of the electron density. Phys. Rev. B. Condens. Matter**37**, 785–789 (1988).

[25] Becke, A. D. Density-functional thermochemistry. III. The role of exact exchange. J. Chem. Phys.**98**, 5648–5652 (1993).

[26] Volpe, V. et al. Toward the Elucidation of the Competing Role of Evaporation and Thermal Decomposition in Ionic Liquids: A Multitechnique Study of the Vaporization Behavior of 1-Butyl-3-methylimidazolium Hexafluorophosphate under Effusion Conditions. J. Phys. Chem. B**121**, 10382–10393 (2017).

[27] Khrizman, A., Cheng, H. Y., Bottini, G. & Moyna, G. Observation of aliphatic C–H···X hydrogen bonds in imidazolium ionic liquids. Chem. Commun.**51**, 3193–3195 (2015).

[28] Dibrov, S. M., Kochi, J. K. "Crystallographic view of fluidic structures for room temperature ionic liquids: 1-butyl-3-methyl imidazolium hexafluorophosphate", Acta Cryst. C62, pp. o19-o21, 2006, doi:10.1107/S0108270105037200.

[29] Panja, S. K. et al. Evidence of C--F-P and aromatic π--F-P weak interactions in imidazolium ionic liquids and its consequences. Spectrochim. Acta Part A Mol. Biomol. Spectrosc.**194**, 117–125 (2018).

[30] Dzyuba, S. V & Bartsch, R. A. New room-temperature ionic liquids with -symmetrical imidazolium cations. Chem. Commun. 1466–1467 (2001) doi:10.1039/B104512C.

[31] Alavi, S. & Thompson, D. L. Molecular dynamics studies of melting and some liquid-state properties of 1-ethyl-3-methylimidazolium hexafluorophosphate [emim][PF6]. J. Chem. Phys.**122**, 154704 (2005).

[32] Gineityte, V. On the relation between the stabilization energy of a molecular system and the respective charge redistribution. J. Mol. Struct. THEOCHEM**585**, 15–25 (2002).

Copyright © 2024 Authors